Thermal Integration of Homogeneous Azeotropic Distillation Sequences

Existing methods for synthesizing thermally-integrated distillation sequences fail frequently when applied to nonideal and azeotropic systems, because increasing the column pressures often introduces new azeotropes and distillation boundaries into the mixture, which make some separation tasks infeasible. A new thermal integration procedure is presented that combines a bifurcation and residue-curve map analysis with the methods of Andrecovich and Westerberg. The procedure is demonstrated with two commercially important separations: ethanol-water-ethylene glycol and methanol-acetone-water. Energy savings of 65% and 40%, respectively, over the optimized nonintegrated sequences are possible.

Jeffrey P. Knapp
Michael F. Doherty
Department of Chemical Engineering
Goessmann Laboratory
University of Massachusetts
Amherst, MA 01003

Introduction

Distillation is the most widely used separation technique in the chemical process industries and typically consumes a third or more of the total energy used in a chemical plant (Linnhoff et al., 1983). In 1976, this represented nearly 3% of the total national energy consumption (Mix et al., 1978). Since few of the mixtures encountered in the chemical process industries are ideal, there is clearly a great incentive to find ways to reduce the amount of energy required to distill nonideal and azeotropic mixtures. This problem, however, has received little attention in the technical literature.

Methods for conserving energy in distillation have been known for at least 40 years (see Robinson and Gilliland, 1950), and there are numerous papers in the literature on this subject. With the notable exception of the papers by Lynn and Hanson (1986), Katzen et al. (1980), and Messick et al. (1983), most of these studies have been limited to constant-volatility mixtures for which simple short-cut design procedures exist. The recent National Research Council report on the critical needs and opportunities in separation and purification (King et al., 1987) identifies the thermal integration of nonideal-mixture separations and processes combining different unit operations such as distillation and extractive distillation as vital research areas and states that "substantial reductions in energy use and novel process combinations can be expected to emerge from fundamental studies in this area." The goal of this paper is to address this need by presenting a systematic procedure for conserving energy in the distillation of nonreacting mixtures containing homogeneous azeotropes.

We restrict our study to simple sharp separators, mixtures with no liquid-phase immiscibilities, and column pressures between 1 and 10 atm (to avoid the higher costs associated with vacuum pressures and the difficulties associated with excessively high temperatures, respectively). Furthermore, the separation system is treated in isolation from the rest of the process. This allows the relevant features of the problem to be identified without needlessly complicating the problem. If desired, our ideas can be combined with the methods of Linnhoff et al. (1983) or Hindmarsh and Townsend (1984) to integrate the separation system into the overall process.

One fundamental difference between the separation of constant-volatility mixtures and azeotropic mixtures is the number of possible ways of separating the mixture. For constant-volatility mixtures the number of possible sequences is large (see Eq. 1 of Thompson and King, 1972). Consequently, many authors (e.g., Rathore et al., 1974; Morari and Faith, 1980; Floudas and Paules, 1988; Kakhu and Flower, 1988) have combined the synthesis and thermal-integration problems, though Stephanopoulos et al. (1982) and Hindmarsh and Townsend (1984) found that these two problems can normally be treated sequentially—first find the best two or three nonintegrated sequences and then thermally integrate them. For nonideal mixtures, the presence of azeotropes and distillation boundaries usually causes the number of feasible sequences to be small. Thus, the problem is not to find the optimal nonintegrated sequence for thermal integration but to find the optimal way to integrate the few feasible sequences. Because of the small solution space, the graphical column-stacking method of Andrecovich and Westerberg (1985a) would seem to be well-suited to this problem.

The Andrecovich and Westerberg Method

The T-Q diagrams and graphical column-stacking concepts presented by Andrecovich and Westerberg (1985a) can also be applied to nonideal and azeotropic separations (within the limitations discussed later). Variations of the Andrecovich and Westerberg method can also be used. For example, Glinos et al. (1985) replace $Q\Delta T$ with ΔS and use $1/T$-Q diagrams instead of T-Q diagrams. These methods provide a rapid technique for fixing the column pressures and estimating the relative merits of the alternative thermally-integrated structures.

The goal of thermally integrating a distillation sequence is to reduce the energy consumption with at worst a small increase in total annualized cost. Therefore, instead of seeking minimum utility sequences which contain a large number of columns, the best way to apply these methods is to use an idea similar to that behind Andrecovich and Westerberg's least-cost tree-search algorithm. Starting with the same number of columns as in the nonintegrated sequence, compare the predicted energy consumptions of the possible column-stacking options and design only the best one or two. Next take the column with the highest utility requirement and split its separation task between two columns by adding a second effect. Again compare the predicted energy consumptions of all the column-stacking options and design only the best one or two. This process can be repeated with a new column added at each stage until the costs start to increase significantly. Other stopping criteria include: the required reboiler temperature exceeds that of the hottest utility; the column pressures are high enough to make the accuracy of the VLE model uncertain; and the integrated sequence is more complex than desired. When making comparisons of the different column-stacking options, remember that the quantity $Q\Delta T$ increases with column pressure. While this does not cause the sequence structure to change, as shown by Andrecovich and Westerberg (1985b), the actual energy consumption of the sequence can be significantly higher than that predicted by assuming a constant value for $Q\Delta T$.

Unfortunately, the Andrecovich and Westerberg method (and the other synthesis/thermal integration methods in the literature) often fails when applied to nonideal and azeotropic mixtures. The reason for this is that increasing the column pressures for thermal integration frequently causes new azeotropes and distillation boundaries to appear that render the sequence infeasible. Additional information is needed to determine which separation tasks become infeasible and at which pressures. The *bifurcation* pressures, found using the method described by Knapp (1990), are the pressures at which new azeotropes appear or at which existing azeotropes disappear. Between each pair of bifurcation pressures, there will be a unique residue-curve map that determines whether the separation is feasible over that pressure range. At each bifurcation pressure, the residue-curve map changes abruptly but then remains globally invariant up to the next bifurcation pressure. [Though the number of azeotropes and hence the global structure of the residue-curve map remains unchanged in each pressure range, the location (composition) of the azeotropes and distillation boundaries may vary with pressure.] Thus, the information needed to determine feasibility can be obtained by first locating the bifurcation pressures and then drawing a representative residue-curve map (see Doherty and Caldarola, 1985 for details) in each pressure range.

Once the feasibility of the separation with changing pressure has been ensured, it is necessary to check that the target product compositions for each column remain obtainable as the column pressure is changed. For constant-volatility mixtures this is always true. However, when there are azeotropes present that change composition with pressure, it is possible that the original target product compositions may lie on the opposite side of an azeotrope or distillation boundary at other pressures and hence have to be changed to remain reachable. The pressure sensitivity of the azeotropes can most easily be determined by drawing residue-curve maps at several pressures (say 1, 5, and 10 atm when the columns are restricted to operate between 1 and 10 atm), *in addition to* those pressures called for by the bifurcation analysis. Armed with this information, the Andrecovich and Westerberg techniques can be applied to discriminate between the remaining integration alternatives.

Since there is more than one way to stack the columns in a sequence for thermal integration and, as will be shown, there can be considerable differences in the energy consumption of different column-stacking configurations of the same separation sequence, it is normally necessary to examine each column-stacking alternative. For constant-volatility mixtures, Andrecovich and Westerberg recommend stacking the columns in order of decreasing volatility of the distillate composition: the most volatile distillate is at the lowest pressure and the least volatile distillate is at the highest pressure. For azeotropic mixtures, however, relative volatility is not a good measure, since the relative volatility of two components not only varies with composition but can actually reverse.

To demonstrate the thermal integration procedure for distillation sequences containing azeotropic mixtures, two separations of commercial importance will be used as examples:

1. The separation of ethanol and water using ethylene glycol as the entrainer.
2. The separation of acetone and methanol using water as the entrainer.

The first mixture does not form any new azeotropes as the pressure is increased, but the second mixture does form a new azeotrope and a distillation boundary at elevated pressure that affects the thermal integration process. After discussing these examples, a generalized algorithm for thermally integrating homogeneous azeotropic distillations will be presented.

Separation of Ethanol from Water Using Ethylene Glycol

The phase-out of *tetra*-ethyl lead as an octane booster and Colorado's recent mandatory oxygenated-fuels program to reduce cold weather carbon monoxide pollution (Anderson, 1987) are creating an increasing market for oxygenated octane enhancers—one of which is ethanol. Furthermore, the most commonly used oxygenate, methyl *tert*-butyl ether (MTBE), is facing a potential challenge from another fermentation-ethanol-based product, ethyl *tert*-butyl ether (Potter, 1989; Anderson, 1988), with the key being the ethanol feedstock price. Thus, reductions in the energy consumption of the ethanol purification process may have a considerable effect on the market for octane enhancers.

A frequently cited drawback to the production of fuel-grade ethanol from renewable grain and biomass sources is that the traditional purification of ethanol by distillation is energy-

intensive, consuming 50 to 80% of the energy used in typical ethanol-producing fermentation processes (Ladisch and Dyck, 1979). Knight and Doherty (1989) show that substantial savings in energy and capital can be achieved by optimizing the separation sequence. Additional energy savings of up to 65% over the optimized sequence are attainable by thermal integration, as will be explained subsequently.

The first step, prior to any design, is to calculate the bifurcation pressures and draw residue-curve maps at several pressures (chosen as described previously) to see: 1. which sequences are feasible at atmospheric pressure; 2. which separation tasks, if any, become infeasible at higher pressures; and 3. which targeted column-product compositions, if any, need to be adjusted as the pressure is changed. Since there are no distillation boundaries at 1 atm (Figure 1a), it would appear plausible by symmetry arguments that either pure ethanol or pure water could be recovered in the extractive column. Exhaustive design calculations, however, indicate that only pure ethanol can be obtained as the distillate. Figure 1b shows that no new azeotropes or distillation boundaries form at elevated pressures. Hence, the separation remains feasible at higher pressures and the thermal integration analysis can proceed.

For comparison with other designs from the literature, approximately 40.1 Gg/yr (13.4 million gal/yr or 88.2 million lb/yr) of 99.8 mol % ethanol will be produced from a 4.2 mol % ethanol fermentation broth via the classical extractive distillation sequence with ethylene glycol as the entrainer (see Figure 2). Provisions for removing the fusel oils and aldehydes present in the fermentation broth are not included but they could be handled in the conventional manner (see Paul, 1980). The fresh feed is assumed to be at the fermenter temperature of 38°C and all streams leaving the separation system are cooled to 49°C. The vapor-liquid equilibrium is modeled by the Van Laar equation using the two sets of interaction parameters given in Knapp (1990), which accurately predict the azeotrope up to 12 atm without the need for vapor-phase fugacity coefficients. All

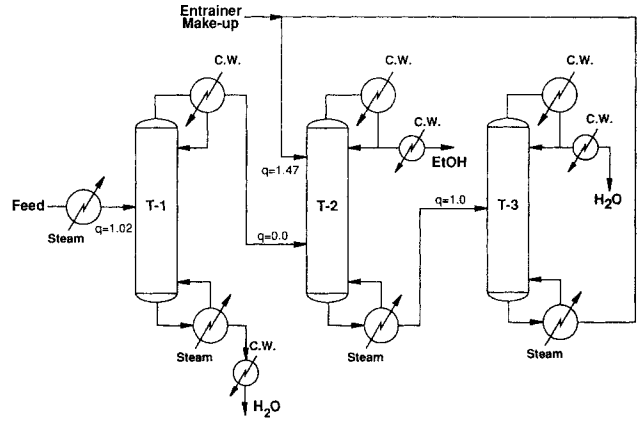

Figure 2. Optimal nonintegrated sequence for purifying ethanol by extractive distillation.

T-1 is the preconcentrator, *T*-2 is the extractive column, and *T*-3 is the entrainer recovery column.

columns are restricted to operate between 1 and 10 atm. The columns are designed using the method of Knight and Doherty (1989) that eliminates the need for recycle convergence schemes. All distillate and reflux streams are at their bubble-point temperatures. Steam is assumed to be available at continuous levels. Cooling water is available at 30°C and is returned at 50°C. The equipment sizing and costing correlations are taken from Knapp (1990) using fourth-quarter 1986 prices.

Prior to thermal integration the sequence should be optimized because, as shown by Minderman and Tedder (1982), extensive optimization can provide savings equal to that of thermal integration. Knight and Doherty (1989) show how a short-cut optimization procedure based on the work of Fisher et al. (1985) can be applied to the same example used here; however, their optimization is incomplete. They conclude that the feed ratio to the extractive column is the only significant optimization variable,

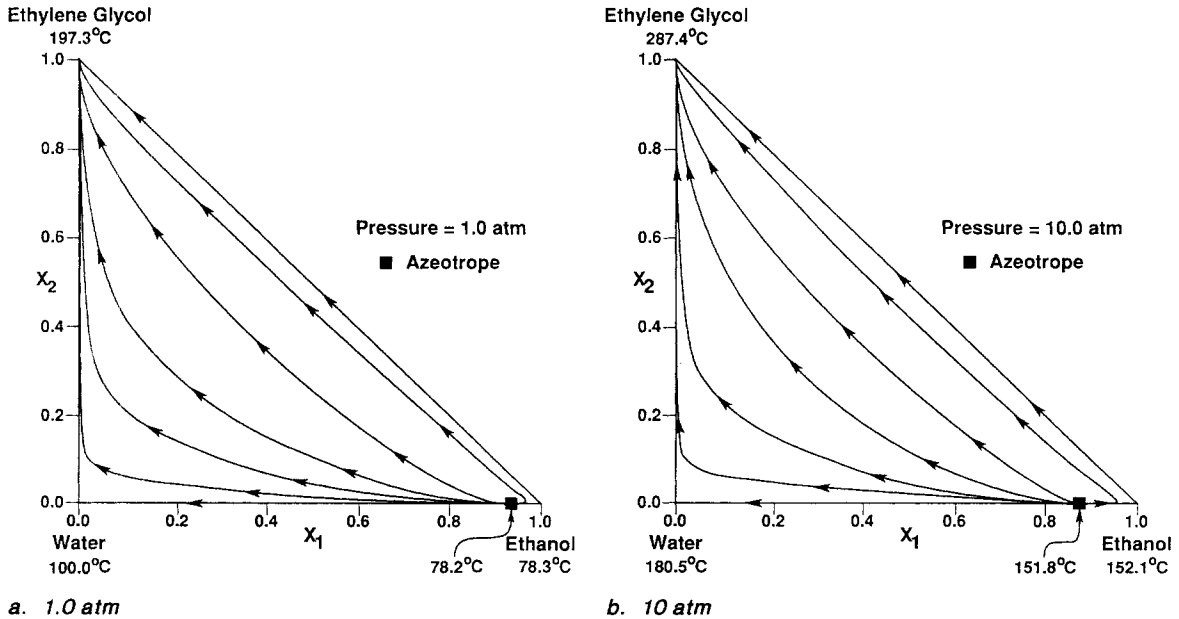

Figure 1. Residue-curve map for ethanol-water-ethylene glycol.

but they come to this conclusion because they do not include the ethanol concentration in the distillate of the preconcentrator and the feed qualities in their list of optimization variables. Actually there are three significant optimization variables:

1. The ratio of the upper to lower feed flow rates
2. The mole fraction of ethanol leaving the preconcentrator (or equivalently, entering the extractive column via the lower feed)
3. The feed quality to the preconcentrator.

The minimum feed ratio necessary to make the separation feasible is 0.19. Logic similar to that of Julka and Doherty (1989) is used to find the value of $x_{D,\text{heavy}}$ ($x_{B,\text{light}}$ for indirect splits) that gives the optimal trade-off between the number of trays and the reflux ratio. Also, as suggested by Lynn and Hanson (1986), a partial condenser is used on the preconcentrator to give a saturated-vapor lower feed to the extractive column. [In all of the thermally-integrated sequences described below, a partial condenser will be used on the preconcentrator whenever the preconcentrator pressure is greater than or equal to the extractive column pressure. Conversely, whenever the extractive column operates at a higher pressure than the preconcentrator, a total condenser will be used on the preconcentrator to avoid the need for a vapor compressor.] This reduces the energy consumption by about 710 kJ/kg (2,000 Btu/gal). Typical column profiles for the extractive column are shown in Figure 5.5 of Knight (1986), and with the constant molar overflow assumption, in Figure 11 of Levy and Doherty (1986). The net effect of performing the more complete optimization (see Table 1) is to reduce the total annualized cost (TAC) by 20% to $2.01 million/yr and the energy consumption by 14% to 7,670 kJ/kg relative to the results reported by Knight and Doherty (1989). [See the Appendix.] This design will serve as the base case for thermal integration.

There are two basic ways to stack the three columns in the sequence for thermal integration (Figure 3). [The areas representing columns on the T-Q diagrams throughout this paper are not rectangles like those used in Andrecovich and Westerberg (1985a), because most feeds are not saturated liquids and a partial condenser is sometimes used on the preconcentrator.] Sequence I (Figure 3b) increases the pressure in the extractive column, and optionally, the entrainer recovery column so that their condensers can drive the reboiler of the preconcentrator. Sequence II (Figure 3c) uses a pressurized preconcentrator to drive the reboiler of the extractive column. Comparing Figures 3b and 3c, it is clear that sequence I has the smaller total width (ΣQ_{Hot}) and hence the smaller predicted energy consumption (about 20% less). At this point, sequence II could be eliminated from the heat-integrated alternatives under consideration, but to illustrate the integration procedure it will not be.

Table 1. Distillation Processes for Producing Fuel-Grade (99.8 mol %) Ethanol: Thermally-Integrated vs. Nonintegrated*

	TAC ($\times 10^6$ \$/yr)	Energy Consumption (kJ/kg EtOH)
Knight and Doherty (1989) Extractive Distillation with Ethylene Glycol. Feed Preheater Added	2.51	8,920
Optimized, Nonthermally-Integrated Extractive Distillation with Ethylene Glycol (Base-Case Design for Thermal Integration Studies)	2.01	7,670
Thermally-Integrated Sequence I** (Figure 4)	2.23	4,160
Thermally-Integrated Sequence II (Figure 3c)	2.37	5,000
Thermally-Integrated Sequence III (Figure 5a)	2.23	4,210
Thermally-Integrated Sequence IV** (Figure 6)	2.36	2,700
Ryan and Doherty (1989) Optimized Heterogeneous Azeotropic Distillation with Benzene. Feed Preheater Added	2.05	10,380

*Feed: 4.2 mol % EtOH at 38°C; Product: 40.1 Gg/yr
**Patent pending

Sequences I and II must be optimized so that a valid comparison can be made with the base-case nonintegrated sequence. Surprisingly, none of the compositions or flow rates (i.e., feed ratio) change from their optimal values in the base case despite the different column pressures. (Feed qualities are not included in this optimization.) This result is analogous to that of Stephanopoulos et al. (1982) for constant-volatility mixtures and suggests that the optimization of each candidate integration alternative can be omitted even for azeotropic mixtures. Upon closer examination this result is not so unexpected. Optimizing the base-case sequence at atmospheric pressure finds the variable values that tend to minimize the equipment size (cost) and utility usage. As long as the azeotropic compositions do not change appreciably with pressure, as in this example (see Figure 1), it seems logical that these same values will continue to result in minimum overall cost. If the azeotropes are pressure-sensitive, however, an optimal stream composition at 1 atm (e.g., the approach to the azeotrope in the distillate from the preconcentrator) could become difficult (i.e., expensive) or impossible to achieve at higher pressures. This is another good reason for drawing a series of residue-curve maps at different pressures prior to thermal integration.

The column-stacking procedure fixes most of the structure of the integrated sequence by determining the major stream matches (the matches between the reboilers and condensers) and implicitly sets the column pressures (condensers must operate at some minimum approach temperature (e.g., 10°C) above the temperature of the reboiler with which they are matched), but numerous options still exist for integrating the streams between columns. Most authors assume that all feed and product streams are saturated liquids and neglect the energy necessary to heat or cool these streams and/or they assume that the heat duties of these streams are much smaller than the latent heat changes associated with reboilers and condensers. Meszaros and Fonyo (1988) cite several examples.

This, however, is not always true. Because the feed stream to the preconcentrator is a subcooled liquid and its flow rate is an order of magnitude larger than the other feed flow rates in the sequence (due, in this case, to the dilute feed composition and the fact that most of the water is removed in the first column), the amount of energy required to heat the feed to the preconcentrator is roughly the same as the duty of the reboiler and condenser of the extractive column. If steam was used to heat this feed instead of stream matching, the energy consumption of the thermally-integrated designs in this paper would be 30–85%

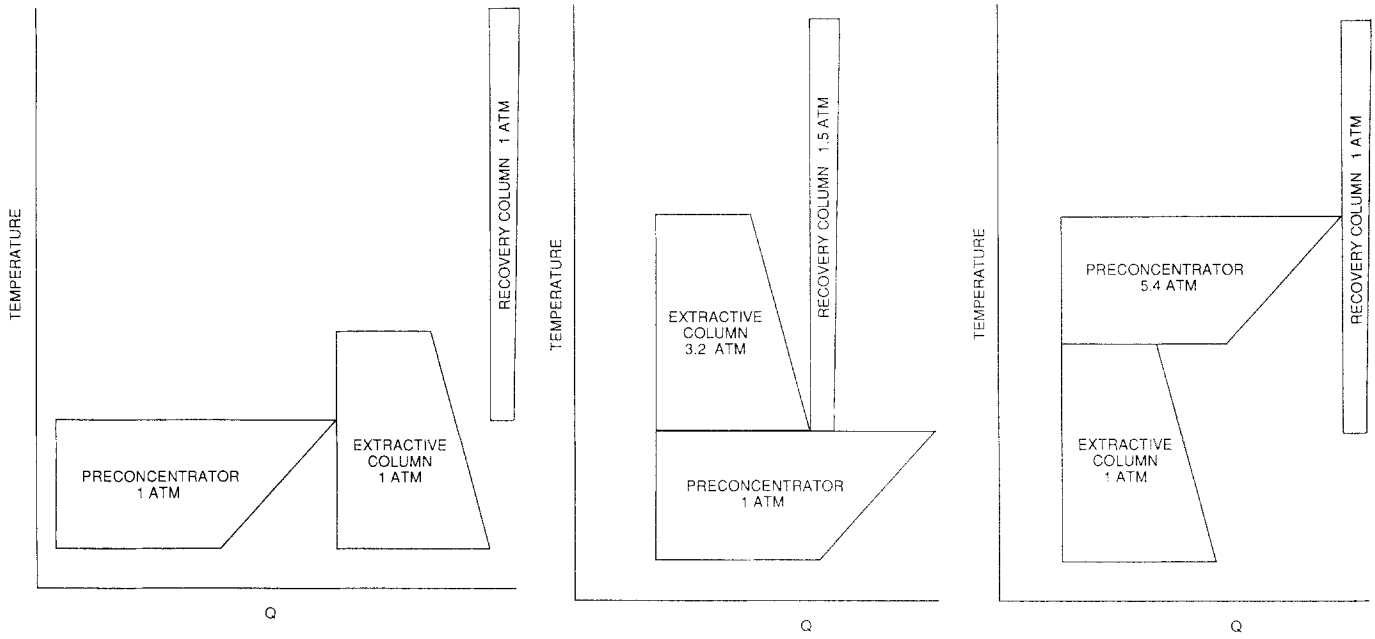

a. Optimized sequence with no thermal integration: $\Sigma Q_{reboiler}$ = 7,970 kW

b. Structure for thermally-integrated sequence I: predicted $\Sigma Q_{reboiler}$ = 4,550 kW assuming constant QΔT

c. Structure for thermally-integrated sequence II: predicted $\Sigma Q_{reboiler}$ = 6,130 kW assuming constant QΔT

Figure 3. *T-Q* diagram for producing fuel-grade ethanol.

The energy needed for feed preheating is not included in the energy consumptions given in the figure captions.

higher. Even though some of the other feeds are significantly subcooled (due to their pressure being changed between columns), none of them have large heat duties (because their flow rates are moderate), so it makes little difference (less than 10%) how they are integrated. This greatly simplifies the thermal integration procedure by reducing the number of alternatives that must be examined and is also in agreement with the results of the previous authors. Other criteria such as controllability or operability can be used to decide how to heat or cool these streams.

If the feed preheating and precooling are to be done by matching with other streams, then the feed qualities cannot easily be included in the short-cut optimization procedure. The attainable q values depend on the particular matching of the streams used and the heat load of these matches. In addition, there are always several ways to match the available streams. Thus, including the feed qualities in the optimization procedure requires the simultaneous optimization of the q values, the stream matching alternatives, and the heat load on each match. Yet the relatively small savings possible do not justify this added effort.

Consequently, some simple guidelines are needed to quickly and easily arrive at very good estimates for the q values and the best stream matching alternative. A good starting point is to try to achieve similar feed qualities to those in the base case by heating feeds as hot as possible (but generally not beyond a saturated vapor) with product, intermediate, or recycle streams. Thus it is better to use the entrainer recycle stream to heat the lower feed to the extractive column in sequence I from $q = 1.12$ to $q = 0.81$ (which is closer to the base-case optimum of $q = 0.0$) than to heat the feed to the entrainer recovery column from $q = 0.93$ to $q = 0.77$ ($q = 1.0$ in the base case). In both sequences I and II, the bottom product stream from the preconcentrator should be used to heat the fermentation-broth feed as hot as possible ($q = 1.01$ vs. $q = 1.02$ in the base case). When the condenser of a double-feed column cannot supply all of the heat needed by the reboiler with which it is matched, there is another way to save energy. By not cooling the upper feed to the double-feed column (or by cooling it less), the duty on the condenser increases, which in turn increases the duty on the match between the condenser and reboiler and thereby reduces the amount of steam needed by the reboiler.

After the thermal integration is complete, sequence I (patent pending) has an energy consumption that is 46% less than the base case with an 11% increase in TAC, while sequence II saves only 35% in energy yet costs 18% more than the base case (see Table 1). [The energy savings quoted throughout this paper are real. The cost increases may or may not be real because they depend on the cost correlations used. Our cost models are meant only for screening process alternatives and are not expected to be more accurate than within about 10% of the true cost. Also, the steam cost correlation used here may not be typical because it assumes that electricity cogeneration is used to produce lower-pressure steam, i.e., lower-pressure steam costs less than higher-pressure steam by an amount equal to the value of the electricity that could be generated by expanding the higher-pressure steam to the lower pressure. This can result in paying more for less energy.] Thus, although the energy consumptions predicted from the T-Q diagrams (Figure 3) based on the base-case values of Q and ΔT (i.e., by assuming Q and ΔT are independent of pressure) underpredict the actual energy requirements, the diagrams do correctly identify sequence I as the preferred sequence. Figure 4 shows the actual T-Q diagram for sequence I and a schematic of the fully-integrated sequence.

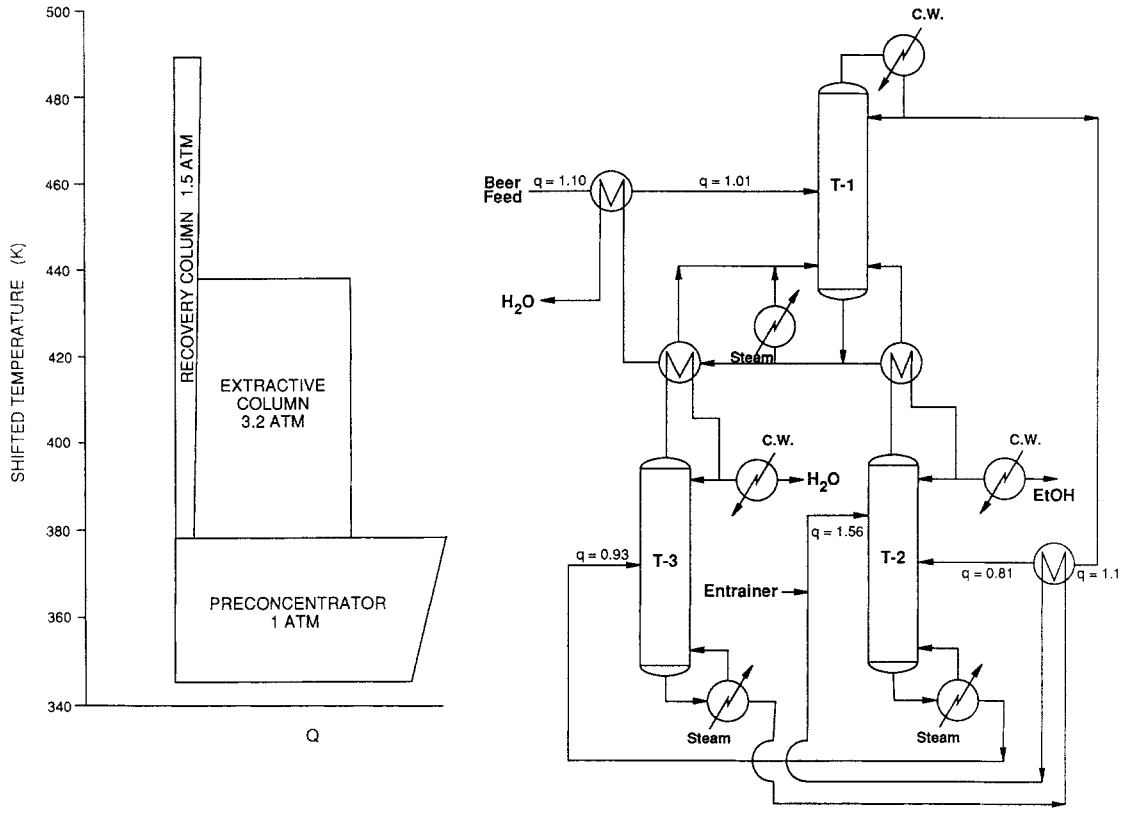

a. Actual T-Q diagram: $\Sigma Q_{reboiler}$ = 5,520 kW

b. Schematic diagram of the sequence: T-1 is the preconcentrator, T-2 is the extractive column, and T-3 is the entrainer recovery column

Figure 4. Thermally-integrated sequence I.

The next step in the integration procedure is to add another column to the sequence by dividing the separation task of the largest energy consumer, the preconcentrator (see Figure 4a), between two columns. There are eight basic ways of integrating the columns in this four-column sequence, even without including the entrainer recovery column in the heat exchanger network (see Figure 5). Fortunately, most of these alternatives can be eliminated without being designed.

The simplest of the eight options is to only integrate the two preconcentrators (Figure 5a). As discussed earlier, it is not necessary to reoptimize this sequence. The guidelines for selecting feed qualities also apply here. The energy consumption can be reduced by 21% by using the bottoms stream from each preconcentrator to heat the column's feed as hot as possible (q = 1.01–1.02) instead of only heating it to the same temperature as the base case. There are negligible differences in energy consumption among the various options for integrating the other feed streams as expected. Partial condensers are used on both preconcentrators (see the earlier comment), causing the lower feed to the extractive column to be slightly superheated (q = 0.0 in the base case). Thus the given guidelines recommend heating the feed to the recovery column with the recycle stream. This indeed turns out to be the best choice. The final version of sequence III uses only 1% more energy and costs no more than sequence I (see Table 1). Thus the addition of the fourth column has a negligible effect on the sequence cost, but sequence III should not be used since it offers no additional energy savings.

By using the condenser and reboiler duties of the columns from the previous three sequences (see Figures 3c, 4a, and 5a), *T-Q* diagrams can be sketched for the next four integration alternatives, enabling these sequences to be immediately eliminated. Since the data used to construct the *T-Q* diagrams are at the same pressures as the columns in these four sequences, the predicted energy consumptions will be quite accurate. The first sequence (Figure 5b) is essentially identical to sequence I except that the preconcentrator has been divided into two effects, both operating at 1 atm. Thus the energy consumption will be identical to that of sequence I. The next sequence (Figure 5c) is related to sequence II. Its energy consumption is about 4,800 kJ/kg—15% higher than that for sequence I. The third sequence (Figure 5d) has an energy consumption of 4,000 kJ/kg. Since this is only a 4% energy savings over sequence I, there is no incentive to pursue this sequence. The fourth sequence (Figure 5e) has the same structure used by Lynn and Hanson (1986) in their four-column sequence but uses different column pressures. The predicted energy consumption is 3,690 kJ/kg. This 11% energy savings over sequence I is not enough to justify designing the sequence since the sequences in Figures 5f and 5h have much lower energy consumptions.

At this point there are only three more sequences to consider—those which stack three columns one on top of the other (Figures

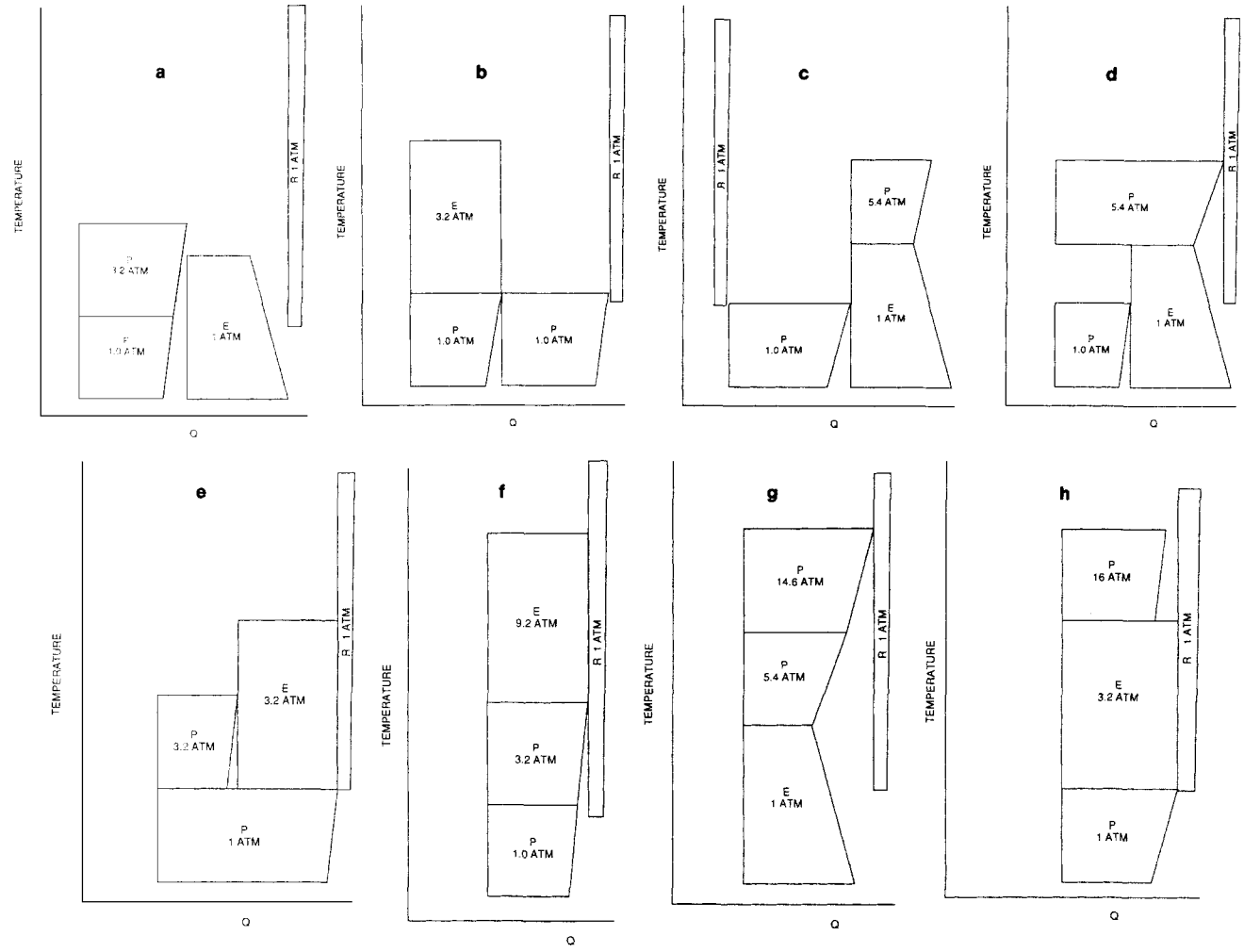

a. Thermally-integrated sequence III: Actual $\Sigma Q_{reboiler} = 5{,}580$ kW
b. Identical to sequence I: predicted $\Sigma Q_{reboiler} = 5{,}520$ kW
c. Predicted $\Sigma Q_{reboiler} = 6{,}730$ kW
d. Predicted $\Sigma Q_{reboiler} = 5{,}310$ kW
e. Sequence structure used by Lynn and Hanson: predicted $\Sigma Q_{reboiler} = 4{,}890$ kW
f. Thermally-integrated sequence IV: actual $\Sigma Q_{reboiler} = 3{,}580$ kW
g. Predicted $\Sigma Q_{reboiler} = 4{,}120$ kW
h. Predicted $\Sigma Q_{reboiler} = 4{,}300$ kW

Figure 5. Eight possible ways to stack the columns in the four-column multieffect sequence.
The entrainer recovery column is not thermally-integrated with the other columns. (Drawings not to scale.) P = preconcentrator, E = extractive column, and R = entrainer recovery column.

5f, 5g and 5h). Of these, only sequence IV (Figure 5f) does not require a column that operates above 10 atm—the maximum allowable pressure. After designing sequence IV, the energy consumption of the last two sequences (Figures 5g and 5h) will be calculated and compared with sequence IV to see if there is an incentive to increase the maximum allowable pressure.

Sequence IV (Figure 6a) stacks the extractive column on top of one of the preconcentrators which in turn is stacked upon the other preconcentrator. Since the extractive column is at a higher pressure, both preconcentrators have total condensers to avoid the need to compress vapors. The feed-quality guidelines again lead to the best design. As in the previous sequences, heating the preconcentrators' feeds with their bottoms stream saves a considerable amount of energy. Because the extractive column condenser cannot supply all the energy needed by the reboiler of the high-pressure preconcentrator, the entrainer recycle stream is cooled only to 110°C before becoming the upper feed. This saves about 330 kJ/kg by making the extractive column condenser duty roughly match the duty of the preconcentrator's reboiler. Integrating the lower feed to the extractive column and the entrainer-recovery-column feed has a negligible effect on the energy usage, though the feed-quality guidelines do yield the option with the lowest consumption. The fully-integrated sequence IV (patent pending) (Figure 6b) has an energy consumption of 2,700 kJ/kg and a total annualized cost of $2.36 million/yr. Including the entrainer recovery column in the

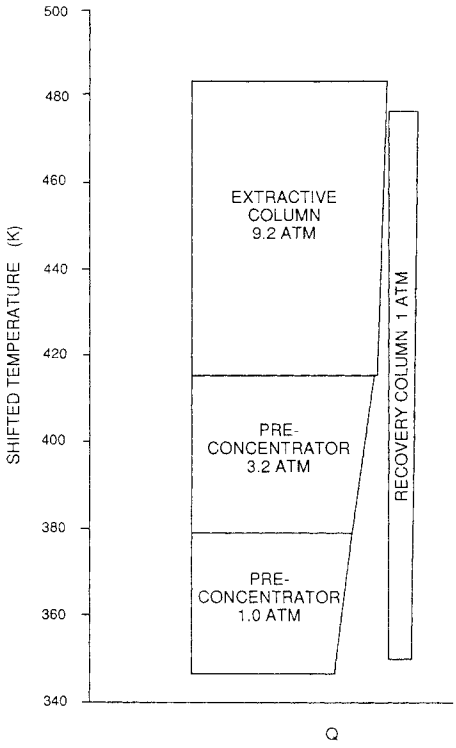

a. T-Q diagram showing sequence structure: $\Sigma Q_{reboiler} = 3{,}580$ *kW*

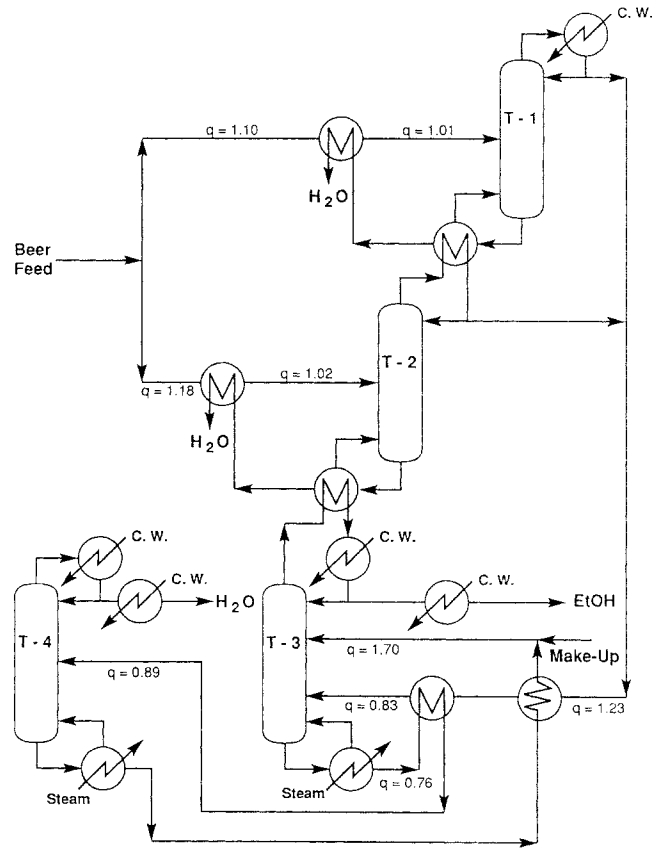

b. Schematic of the sequence structure: T-*1 and* T-*2 are the preconcentrators;* T-*3 is the extractive column; and* T-*4 is the entrainer recovery column*

Figure 6. Thermally-integrated sequence IV (patent pending).

thermal integration adds complexity with only negligible additional energy savings.

The last two integration alternatives (Figures 5g and 5h) require preconcentrator column pressures of 14.6 and 16 atm. To accurately estimate the energy consumption of these sequences, the reboiler and condenser temperatures and heat duties of these high-pressure preconcentrators must be known. According to Andrecovich and Westerberg (1985a), the heat duties, Q, and the temperature difference between the top and bottom of the columns, ΔT, both increase roughly linearly with column temperature. The heat duties and column ΔT's for the preconcentrators in the four sequences studied here in detail can be accurately described by linear functions of the condenser temperature, the reboiler temperature, or the logarithm of the column pressure. (These correlations predicted the heat duties and column ΔT to within 5% of the actual values for a preconcentrator operating at 10 atm.) Using these correlations and the heat duties of columns operating at the same pressures from the previous sequences, the predicted energy consumptions are approximately 3,330 kJ/kg for the sequence with the two preconcentrators stacked on top of the extractive column (Figure 5g) and about 3,240 kJ/kg for the sequence with the extractive column in the middle (Figure 5h)—both higher than that for sequence IV. Furthermore, the reboiler temperatures of the high-pressure preconcentrators in these sequences are well above the limit of 127°C, where the solids in the feed cause severe fouling of the heat-exchange surfaces (Collura and Luyben, 1988). *Thus, the best sequence is alternative IV.*

The next step in the integration procedure would be to add another effect. However, since there is no column whose heat duty is much larger than the others (see Figure 6a), there is no advantage to adding the extra column and the integration procedure is complete,

One additional comment is in order. All the sequence design alternatives presented above were calculated at the economically optimum feed ratio of 0.5. However, Andersen et al. (1989) indicate that the column may be difficult to operate and control at this point. Therefore, a feed ratio of roughly 1.0 may be preferred. For this reason, another sequence was designed using the same structure as sequence IV but with a feed ratio of 1.0. This sequence has a TAC of $2.46 million/yr (4% higher than that for sequence IV) and an energy consumption of 2,715 kJ/kg—only 0.5% more than that for sequence IV. This is not unexpected since, as shown in Figure 7 of Knight and Doherty (1989), there is only a small cost difference between the optimum feed ratio and a feed ratio of 1.0.

Comparison with Other Separation Techniques

By following a systematic procedure we are able to develop a simple sequence that achieves great energy savings at small

additional cost. With an energy consumption of 2,700 kJ/kg and a TAC of $2.36 million/yr, sequence IV represents a 65% savings in energy over the optimized nonintegrated sequence (see Table 1) with a 17% increase in cost (see the earlier comment about the reported costs). [Many actual ethanol plants are considerably larger than the one used in this example, so several of the sequence designs discussed above were scaled up as high as 600 Gg/yr (200 million gal/yr). At this production rate, the annualized separation cost is as low as 10.5–11¢/gal.] This is also 74% less energy at a 15% higher cost than required by the most commonly used method for producing anhydrous fuel-grade ethanol, heterogeneous azeotropic distillation (see Ryan and Doherty, 1989). [See the Appendix.] The same thermally-integrated structure can also be used to produce very high-purity (99.998 mol %) ethanol from the same feed stream (the optimal feed ratio increases to 0.6 and the number of trays in the extractive column becomes large). This thermally-integrated high-purity sequence costs about 37% less than Black and Ditsler's (1972) long-accepted design and consumes 84% less energy (Table 2). (Black and Ditsler's column specifications with a preconcentrator and feed preheater added were run through our design procedure.)

Of the many proposed purification processes for producing ethanol (Ladisch and Dyck, 1979; Black, 1980; Katzen et al., 1980; Eakin et al., 1981; Douglas and Feinberg, 1983; Messick et al., 1983; Barba et al., 1985; Lynn and Hanson, 1986; Ryan and Doherty, 1989), only solvent extraction with an "ideal" solvent (Eakin et al., 1981), the combination of distillation and dehydration using cellulose (Ladisch and Dyck, 1979), multieffect extractive distillation (Lynn and Hanson, 1986), and possibly the A.D. Little CO_2 extraction process (Eakin et al., 1981) can approach this low energy requirement (Table 3). However, these four techniques need to be examined more closely.

The solvent extraction process with an "ideal" solvent is actually a hypothetical process because no such solvent has yet been found (Eakin et al., 1981).

Ladisch and Dyck (1979) made a significant error when they calculated the energy consumption for the distillation part of their process. They claim that distilling a 12 wt. % EtOH saturated-liquid mixture into an 84.8 wt. % EtOH product at $1.5r_{min}$ (no fractional recovery is given) requires about 2,440 kJ/kg. Figure 3 of Eakin et al. (1981) indicates that this separation (with an unknown feed quality, fractional recovery, and r/r_{min}) requires 3,710 kJ/kg, while our calculations (with $r/r_{min} = 1.5$, a saturated-liquid feed, and a 99% fractional recovery) say that the separation requires 4,800 kJ/kg or 6,950 kJ/kg with the feed preheater included. Thus the energy consumption for the combined distillation/desiccation process should be 4,140–5,240 kJ/kg or 7,390 kJ/kg including the preheater.

Lynn and Hanson (1986) use the same four-column sequence structure as that shown in Figure 5e, yet their sequence consumes less energy than the sequence in Figure 5e (Table 3). There are two reasons for this:

Table 2. Extractive Distillation Processes Using Ethylene Glycol for Producing High-Purity (99.998 mol %) Ethanol: Thermally-Integrated vs. Nonintegrated

	TAC ($\times 10^6$ $/yr)	Energy Consumption (kJ/kg EtOH)
Black and Ditsler (1972) Preconcentrator and Feed Preheater Added	4.26	16,480
Optimized, Nonthermally-Integrated Sequence	2.34	7,740
Thermally-Integrated Sequence Same Structure as Thermally-Integrated Sequence IV	2.67	2,700

Table 3. Alternative Technologies for Ethanol Purification*

Process	Energy Consumption (kJ/kg EtOH)	Concentration Range (wt %)
*Ladisch and Dyck (1979)***	2,870	12–99.8
Combined Distillation/Dessication Process Using Cellulose		
Eakin et al. (1981)		
CO_2 Extraction	2,820–3,530	10–100
Solvent extraction with an "Ideal" Solvent†	1,270	10–100
Douglas and Feinberg (1983)		
Solvent Extraction	6,280	10–98
Membrane Pervaporation	4,600	8.0–99.5
Barba et al. (1985)		
Distillation with Ionic Salts	5,020	7.5–99
Black (1980)		
Vacuum Distillation	12,840	6.4–98
Azeotropic Distillation		
Pentane	10,910	6.4–99.9997
Benzene	12,250	6.4–99.9992
Diethyl Ether	13,670	6.4–99.990
Extractive Distillation		
Gasoline	10,260	6.4–Gasohol
Ethylene Glycol	34,100[*sic*]	6.4–99.9992
Katzen et al. (1980)		
Thermally-Integrated Heterogeneous Azeotropic Distillation	6,360	7.1–99.19
Messick et al. (1983)	4,160–5,340	Dilute to Anhydrous
Thermally-Integrated Heterogeneous Azeotropic Distillation		
Lynn and Hanson (1986)		
Multieffect Extractive Distillation with Ethylene Glycol 4-Column Sequence (2-Effects,	2,730	10–99.9
2 Vacuum Columns)	3,300	6–99.9
Thermally-Integrated Extractive Distillation with Ethylene Glycol		
Base Case (No Integration)	7,670	10–99.9
	10,780	6–99.9
Thermally-Integrated Sequence IV‡	2,700	10–99.9
	3,720	6–99.9
Integrated Sequence IV with Saturated-Vapor Feed and 2 Vacuum Columns	1,870	10–99.9

*These may not be optimum designs and they may not start with the feed at the fermenter temperature.
**The reported energy consumption is incorrect, as explained in the text.
†This is a theoretical process; no "ideal" solvent has yet been found.
‡Patent pending.

1. Lynn and Hanson use a saturated-vapor lower feed to the extractive column (made possible by using the overhead vapor of the low-pressure preconcentrator to provide the reflux to both preconcentrators).

2. They use lower column pressures (including two vacuum columns) and, as previously discussed, the condenser and reboiler duties increase with pressure.

When their four-column sequence is compared with our best sequence, seqence IV, we find that they both consume about the same amount of energy. However, since vacuum distillation is more costly than distillation at or above atmospheric pressure, Lynn and Hanson's sequence will undoubtedly cost more than sequence IV. In addition, when the two sequence structures are compared at similar pressure levels, sequence IV is clearly the less energy-intensive. Lynn and Hanson (1986) also present a five-column, three-effect sequence with two vacuum columns. This sequence has a lower energy consumption than their four-column sequence, but it is not included here because it is not clear whether the design is too complex to be either economical or practical. Regardless of the practicality of their five-column sequence, sequence IV has a 12% lower energy consumption when a vapor feed is used and the columns operate at the same vacuum pressures used by Lynn and Hanson (1986).

Lastly, the CO_2 extraction process requires slightly more energy than our sequence IV and will be more costly than distillation because of the high pressures required (60–70 atm) and the need for a gas compressor (Eakin et al., 1981).

In conclusion, contrary to popular opinion, *a well designed extractive distillation process is still the most attractive method for separating aqueous ethanol mixtures.* The cost effectiveness over competitive nondistillation separation techniques increases with increased production rate. The ethanol-water mixture is the only azeotropic mixture for which such detailed comparisons can be made, but we believe these results remain true for a large number of azeotropic separations.

Separation of Acetone and Methanol Using Water

The standard industrial method for separating acetone from methanol is by extractive distillation with water. The vapor-liquid equilibrium for this system is modeled by the Van Laar equation using the interaction parameters given in Knapp (1990). This one set of interaction parameters accurately predicts the azeotropic composition up to 11 atm without the need for vapor-phase fugacity coefficients.

Again, the first step is to calculate the bifurcation pressures and draw a series of residue-curve maps at representative pressures. At atmospheric pressure there is a single binary azeotrope between acetone and methanol (Figure 7a). The bifurcation analysis indicates that 3.51 atm is a bifurcation pressure. In other words, the structure of the residue-curve map changes at 3.51 atm. At this pressure a new minimum-boiling binary azeotrope forms between acetone and water, causing a distillation boundary to appear that puts pure acetone into a different distillation region than pure methanol and pure water. The new azeotrope and distillation boundary are more easily seen at a higher pressure (Figure 7b). This means that it becomes impossible to separate a mixture into pure acetone and an essentially binary mixture of methanol and water above 3.5 atm. Therefore, *before doing any column design calculations and with minimal effort, we know that the acetone must be recovered in a column operating below 3.5 atm.* As will be shown below, this cuts the number of feasible thermal integration alternatives which must be investigated in half. There are no more bifurcation pressures in the allowable pressure range, so no more separation tasks become infeasible at higher pressures. Note that the acetone-methanol binary azeotrope is quite

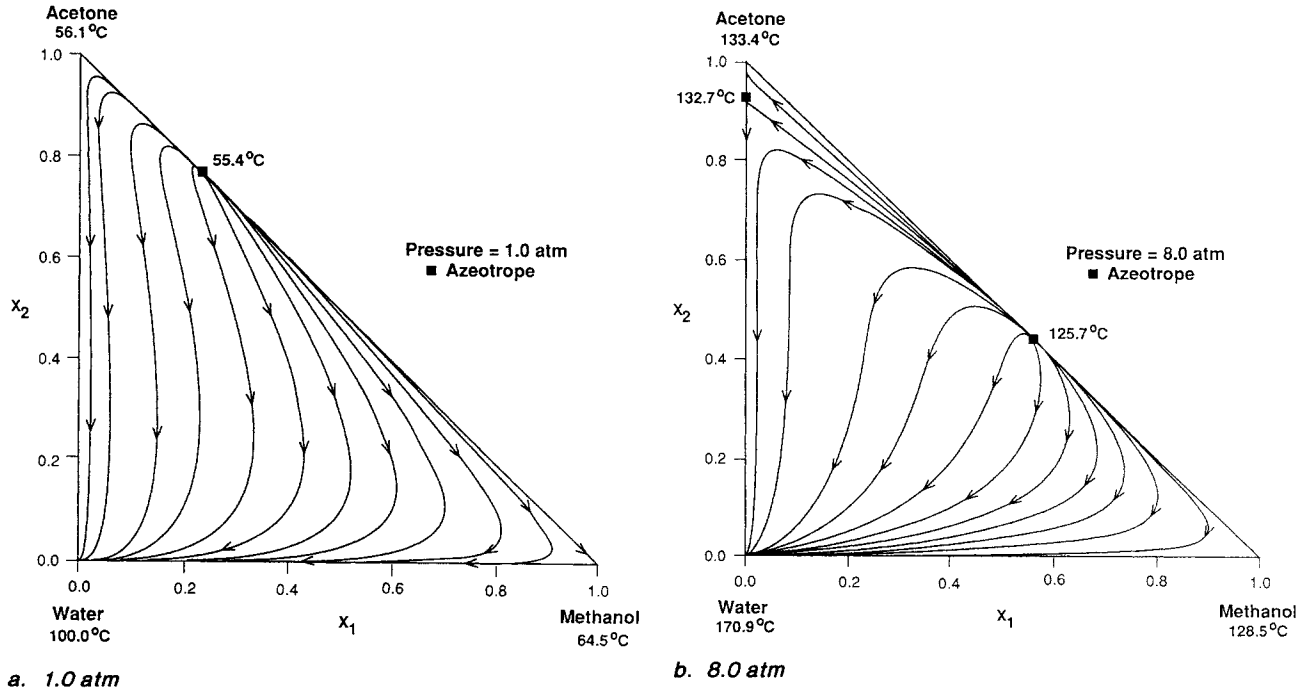

Figure 7. Residue-curve maps for the mixture acetone-methanol-water.
Note the appearance of the acetone-water azeotrope and a distillation boundary.

pressure-sensitive (Figures 7a and 7b), indicating that care must be taken to ensure that all column-product compositions remain obtainable as the column pressure is varied.

Now the sequence design can begin. Since there is no distillation boundary at 1 atm, the residue-curve map for this mixture is similar to that of the ethanol-water-ethylene glycol example, making it again appear plausible by symmetry arguments that either pure methanol or pure acetone can be recovered in the extractive column. However, exhaustive design calculations indicate that only pure acetone can be obtained as the distillate in the first (extractive) column at this pressure. The methanol is recovered in the distillate of the second (entrainer recovery) column (see Figure 8).

For this study, approximately 204.4 Gg/yr of a saturated-liquid, equimolar, binary, acetone-methanol mixture will be separated into 131.7 Gg/yr of 99.5 mol % acetone and 72.7 Gg/yr of 99.5 mol % methanol. The fractional recovery of each of these components is 99.9%. Like the previous example, all columns are restricted to operate between 1 and 10 atm, the distillate and reflux streams are liquids at their bubble-point temperatures, all streams leaving the separation system are cooled to 49°C, and the Knight and Doherty (1989) design method is used. The same utilities and equipment sizing and costing correlations used in the first example are also used here.

The nonintegrated sequence is first optimized using the method outlined in Knight and Doherty (1989). For this example, the feed ratio (the ratio of the upper to lower feed flow rates in the extractive column) is the only dominant optimization variable. (If the feed had been dilute and/or substantially subcooled there may have been other important optimization variables as in the previous example.) The minimum feed ratio is 0.14 and the economically optimal value is 0.55. Because of questions raised about the operability and controllability of columns operating at such low feed ratios (Andersen et al., 1989), all of the sequence design and thermal integration calculations were repeated at a feed ratio of 1.0. There is only about a 4% cost penalty for using the higher feed ratio which is entirely due to the larger columns required to handle the additional entrainer flow since, surprisingly, the energy consumption is 2–10% less than when the feed ratio is 0.55. The values of all of the variables used in the optimal design are given in Table 4 and a schematic of the sequence structure is shown in Figure 8. (An interesting feature to note is that the optimal composition of the highest boiling component in the distillate of the extractive column is greater than that of the intermediate-boiling component.) The column profile for the extractive column is shown in Figure 9. The TAC is \$2.70 million/yr with an energy consumption of 3,190 kJ/kg of acetone. When the feed ratio is 1.0 the TAC is \$2.79 million/yr and the sequence consumes 3,120 kJ/kg of acetone. This optimized nonintegrated sequence (and the corresponding sequence with a feed ratio of 1.0) will serve as the base case for the thermal integration study. The *T-Q* diagram for this base case design is shown in Figure 10a.

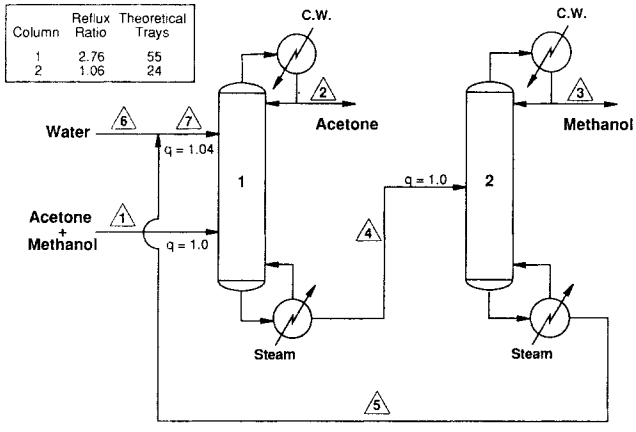

Figure 8. Optimal nonintegrated sequence for separating acetone and methanol by extractive distillation with water (feed ratio = 0.55).

Column 1 is the extractive column and column 2 is the methanol or entrainer recovery column. (See Table 4 for the stream compositions).

There are two thermal integration alternatives for this sequence. Sequence A (Figure 10b) increases the pressure in column 2 so that it can be stacked on top of the first column. Sequence B (Figure 10c) pressurizes the extractive column (column 1) so that it can be stacked on top of the second column. The predicted energy consumptions (assuming constant $Q\Delta T$) for both of these alternatives are similar so neither can be eliminated from consideration. However, sequence B requires the extractive column, which produces the acetone product, to operate at about 5 atm while the bifurcation/residue-curve map analysis indicates that acetone must be purified in a column operating below 3.5 atm. *Therefore, sequence B is infeasible because of the new azeotrope and distillation boundary that appear at elevated pressures; and, without any column design calculation, the bifurcation/residue-curve map analysis has eliminated all single- and multiple-effect thermal integration alternatives which require the extractive column to operate above 3.5 atm.*

To make a valid comparison with the base-case nonintegrated sequence, sequence A must be optimized. According to the reoptimization arguments presented in the first example, special care should be taken because the composition of the acetone-methanol azeotrope changes considerably with pressure. However, because the extractive column (where the acetone-methanol azeotrope movement might cause problems) operates at 1 atm, none of the optimal compositions or flow rates in sequence A change from their base-case values. (Feed qualities are not included in this reoptimization step.) If the sequence feed had contained only a small amount of acetone and a preconcentrator was used to produce a near azeotropic distillate of roughly 78 mol % acetone at 1 atm, then this composition would have to be reoptimized if the preconcentrator was pressurized to say 2.5 atm where the azeotrope is about 65 mol % acetone because the former distillate composition now lies on the far side of the azeotrope at this new pressure. Similarly, the target product compositions and feed ratio for the extractive column would have to be checked if this column was pressurized.

The only decision left to be made is how to match the various feed, product, and recycle streams for the maximum energy savings. Since none of the flow rates are much larger than the others there is only a 1–2% difference between the various stream matching possibilities, but once again the feed preheating guidelines presented in the previous example are applicable. The sequence feed stream is already a saturated liquid so that only leaves the recycle stream and the feed to the second column

Table 4. Optimal Design Variables for Producing 99.5 mol % Acetone: Feed Ratio = 0.55

Stream No.	Flow Rate kmol/h	Mole Fraction			Temp. °C
		Acetone	Methanol	Water	
1	540.0	0.5000	0.5000	0.0000	56.4
2	271.1	0.9950	0.0010	0.0040	49.0
3	271.1	0.0010	0.9950	0.0040	49.0
4	565.9	4.79×10^{-4}	0.4769	0.5226	74.0
5	294.8	1.0×10^{-10}	0.0005	0.9995	100.0
6	2.2	0.0000	0.0000	1.0000	38.0
7	297.0	9.93×10^{-11}	4.96×10^{-4}	0.9995	77.0

to be thermally integrated. The best choice is to heat the feed to column 2 as hot as possible ($q = 1.01$ vs. $q = 1.0$ in the base case) by heat exchange with the entrainer recycle stream.

After the thermal integration is complete, the final version of sequence A has an energy consumption that is about 40% less than the base case with less than a 1% increase in TAC (see Table 5 and the earlier comment concerning the reported costs and energy consumptions). The energy savings is 44% with a 2% lower cost when the feed ratio is 1.0. Figure 11 shows the actual *T-Q* diagram for sequence A and a schematic of the fully integrated sequence.

Since the extractive column (column 1) requires more heat than can be supplied by the second column, the next step in the thermal integration procedure is to add another column to the sequence by dividing the extractive distillation task between two columns operating in parallel. Because the acetone separation becomes impossible above 3.5 atm, the only feasible way to thermally integrate these three columns is to stack one extractive column on top of the other with the entrainer recovery column on top of both (Figure 12). This sequence requires one of the extractive columns to operate at atmospheric pressure and the other to operate at 2.5 atm (2.7 atm for a feed ratio of 1.0) with the entrainer recovery column at 5 atm (6 atm for a feed ratio of 1.0). The predicted energy consumption for this sequence, sequence C, is about 1,320 kJ/kg of acetone, 32% less than for sequence A. (The predicted savings is 16% or 1,460 kJ/kg when the feed ratio is 1.0). However, there is another phenomenon taking place which makes this sequence impractical.

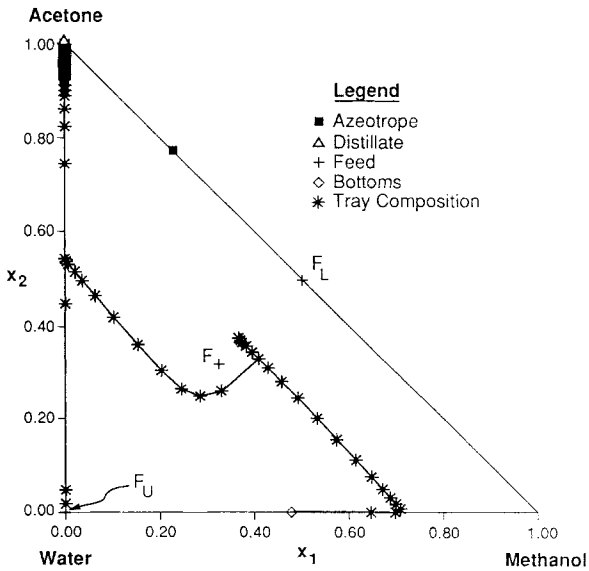

Figure 9. Column profiles for the extractive column at 1.0 atm.

The Feed ratio is 0.55 and the reflux ratio is 2.76. (See Figure 8 and Table 4).

The rectifying section of the extractive column, which is essentially a binary acetone-water mixture (see Figure 9), contains a tangent pinch at atmospheric pressure which becomes more and more pronounced as the pressure increases (i.e., the value of the minimum reflux caused by the tangent pinch and the number of trays required at a fixed multiple of the minimum reflux gets higher and higher) until they both become infinite at the pressure where the position of the binary azeotrope that first appears at 3.51 atm is the same as the distillate composition (99.5 mol % acetone), i.e., the separation becomes infeasible (see Figure 13). In general, when the mixture cannot be approximated as a binary mixture, it is the position of the distillation boundary that causes the separation to become infeasible. Similarly, when an azeotrope disappears at a higher pressure, tangent pinches will exist above that pressure and become less and less severe and the number of trays required will decrease as the pressure is further increased. Therefore, whenever the bifurcation analysis indicates that the number of azeotropes is changing at a certain pressure, care should be taken during the synthesis of thermal integration alternatives to avoid operating the column(s) performing the affected separation task(s) at pressures near the bifurcation pressure where tangent pinches will be severe. For the acetone-methanol-water example, this means that the extractive distillation separation task should not take place much above atmospheric pressure. Sequence C requires one extractive column to operate at about 2.5 atm. At this pressure, the minimum reflux is 6.40 (vs. 2.32 at 1 atm) and the separation requires 136 theoretical trays at $1.2r_{min}$. Clearly the large number of trays required makes sequence C impractical.

Thermal-Integration Algorithm

The results of this work can be summarized in the form of a generalized algorithm for the thermal integration of homogeneous azeotropic distillations. The concepts presented are general and should be readily extendable to multicomponent mixtures.

• *Step 1.* Calculate the bifurcation pressures (see Knapp, 1990) and then draw a series of residue-curve maps at different pressures (see Doherty and Caldarola, 1985, for details) including at least one map between each pair of bifurcation pressures. The technique from Knapp (1990) can be used to predict the

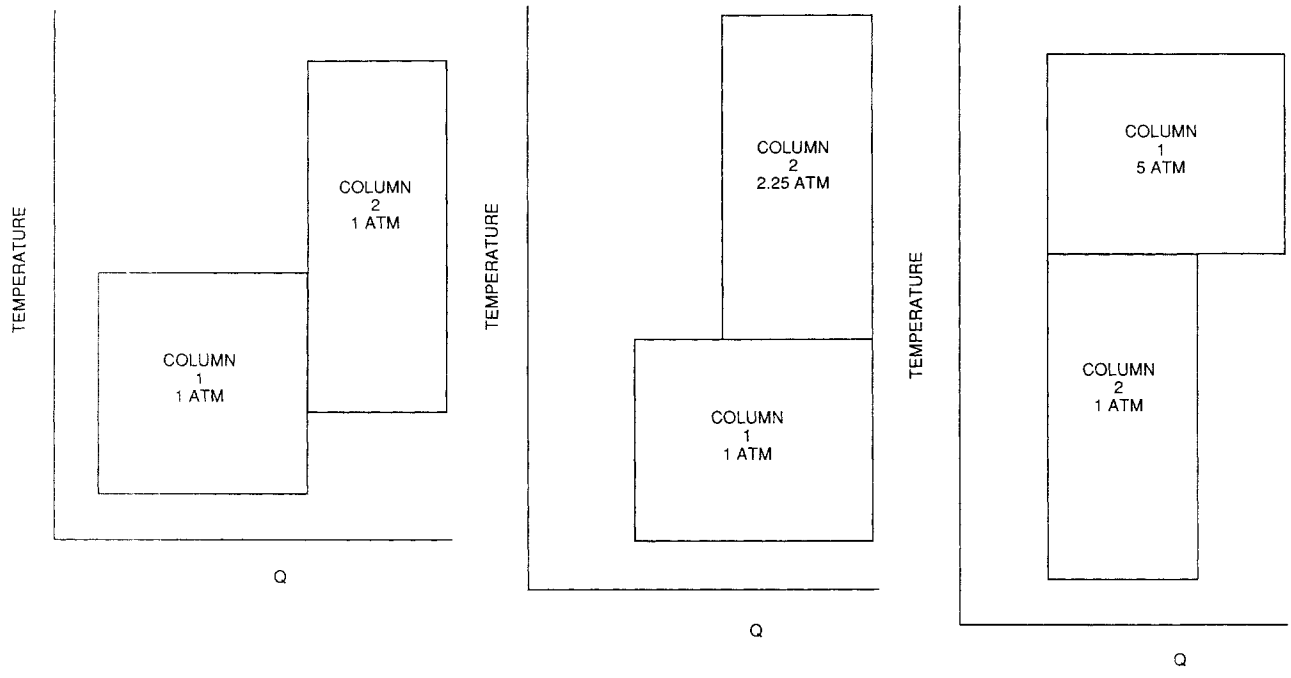

a. Optimized sequence with no thermal integration: $\Sigma Q_{reboiler}$ = 13,840 kW

b. Structure for thermally-integrated sequence A: predicted $\Sigma Q_{reboiler}$ = 8,390 kW

c. Structure for thermally-integrated sequence B: predicted $\Sigma Q_{reboiler}$ = 8,360 kW

Figure 10. *T-Q* diagram for producing 99.5 mol % acetone (feed ratio = 0.55).

Predictions assume constant $Q\Delta T$. Column 1 is the extractive column and column 2 is the methanol or entrainer recovery column.

effect of changing pressure on the azeotropic compositions. Compare the predicted azeotropic compositions against available experimental values. Use more than one set of VLE parameters, if necessary, to accurately describe the system over the pressure range of interest. These residue-curve maps show: 1. which, if any, sequences are feasible at atmospheric pressure (see Figure 10 of Doherty and Caldarola, 1985); 2. whether the mixture is a candidate for pressure-swing distillation (see Knapp and Doherty, 1987); and 3. which separation tasks, if any, become much more (less) difficult or infeasible (feasible) at higher pressures due to the appearance (disappearance) of azeotropes and distillation boundaries.

Table 5. Extractive Distillation Processes for Separating Acetone and Methanol with Water: Thermally-Integrated vs. Nonintegrated

	TAC ($\times 10^6$ \$/yr)	Energy Consumption (kJ/kg EtOH)
Feed Ratio = 0.55		
Optimized, Nonthermally-Integrated Sequence (Base-Case Design for Thermal Integration Studies)	2.70	3190
Thermally-Integrated Sequence A (Figure 11)	2.72	1950
Feed Ratio = 1.0		
Optimized, Nonthermally-Integrated Sequence (Base-Case Design for Thermal Integration Studies)	2.79	3120
Thermally-Integrated Sequence A	2.73	1750

• *Step 2.* For each feasible sequence at 1 atm, determine the minimum feed ratio and specify values for the design variables and initial guesses for the optimization variables as described in Knight and Doherty's (1989) algorithm. As a starting point, set $q = 1$ (saturated liquid) for all the column feeds, i.e., no heating or cooling of the feeds between columns. There are two exceptions: 1. set $q = 0$ (saturated vapor) and use a partial condenser on the previous column when the component appearing in the distillate comprises a large fraction of the feed (Lynn and Hanson, 1986; Meszaros and Fonyo, 1988); and 2. set q = 1.1–1.4 (subcooled liquid) for the upper feed to the extractive column.

• *Step 3.* Design and optimize the sequence(s) as described by Knight and Doherty (1989) and Julka and Doherty (1989). The relative ranks of the variables will quickly narrow the list down to a small number of important optimization variables. If none of the azeotropes in the mixture is pressure-sensitive, the optimization will not need to be repeated as the column pressures are varied for thermal integration. If one or more of the azeotropes is pressure-sensitive, then only those variables affected by the changing azeotropic composition need to be reoptimized at each column pressure.

This optimized design will serve as the base case for thermal integration.

• *Step 4.* Using the reboiler and condenser duties and column ΔT's from the base-case design, sketch *T-Q* diagrams for all the possible ways in which the columns from the base case can be stacked. Include those options which become feasible at elevated

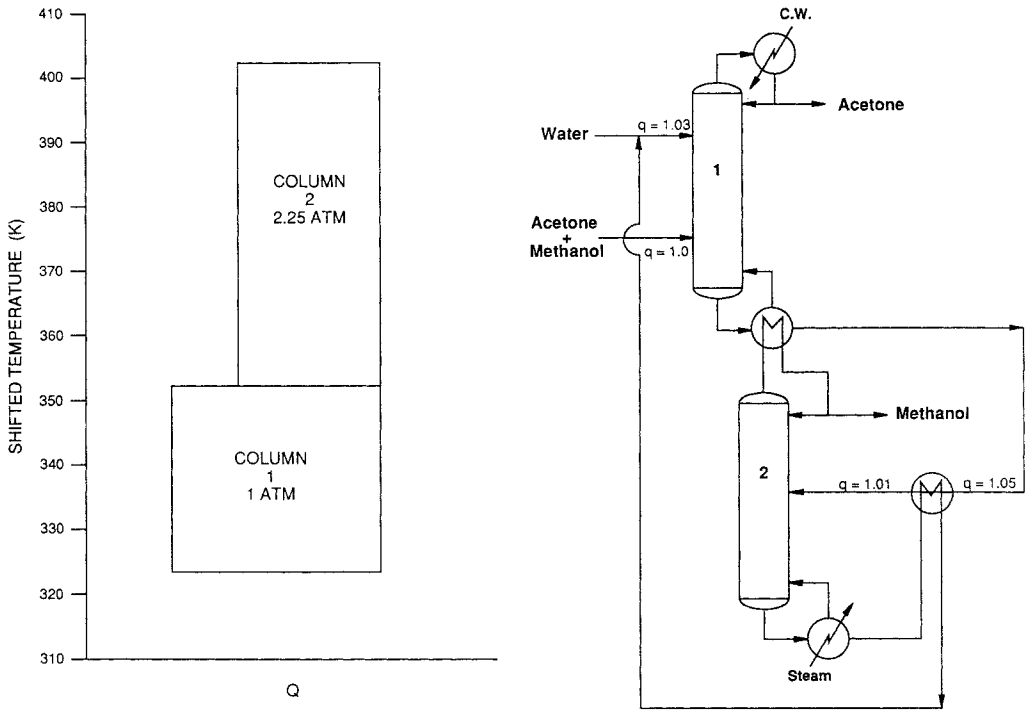

a. Actual T-Q diagram: $\Sigma Q_{reboiler} = 8{,}460$ kW

b. Schematic of sequence structure. All compositions and flow rates are identical to those in Table 4

Figure 11. Thermally-integrated sequence A (feed ratio = 0.55).
Column 1 is the extractive column.

pressures as determined in step 1. Compare the predicted energy consumptions of the various integration alternatives and discard all but one or two of the lowest energy-consuming sequences. In general, if two column-stacking options have similar predicted utility usages, favor the one with the lower column pressures. Since the column heat duties increase with pressure, the predictions underestimate the actual energy consumption more as the column pressure increases.

• *Step 5.* Set the column pressures so that the condensers operate at some minimum approach temperature (e.g., 10°C) above the reboilers with which they are matched. Eliminate the integration alternatives containing separation tasks which are infeasible or extremely difficult because the required column pressures are near or above the bifurcation pressure affecting those separation tasks. Design the remaining sequence(s) with the lowest predicted energy consumption(s).

From the base-case design, identify any column feeds whose heat duty is of the same order of magnitude as the condenser or reboiler duties. It is important to include such feed streams in the heat exchanger network. The other column feeds will have a small effect on the sequence energy consumption. Heat or cool the column feeds by matching them with product, intermediate, or recycle streams. Try to achieve similar feed qualities to those in the base-case design. A hot (less subcooled) upper-feed to a double-feed column will save energy when the double-feed column's condenser duty is less than the duty of the reboiler with which it is matched.

Reoptimize only those variables affected by the moving azeotropes as discussed in step 3.

Calculate the cost and energy consumption of the columns and heat exchangers.

• *Step 6.* Add another column to the sequence by splitting the separation task of the largest energy-consuming column between two effects. Check that no column must operate near or exceed a relevant bifurcation pressure. Predict the energy consumption of all the remaining thermal-integration alternatives. To improve the accuracy, whenever possible base the predictions on data from columns operating at the same or similar pressures. When design data are available for the same separation (and condenser type) at several pressures, correlate the values of the reboiler duty, the condenser duty, and the column ΔT as linear functions of the condenser temperature, the reboiler temperature, and the logarithm of the column pressure to accurately predict the heat duties and column ΔT's at other pressures (temperatures). Retain only the alternatives with the lowest predicted energy consumptions that do not violate physical or user-imposed constraints. Repeat step 5.

• *Step 7.* Repeat step 6 until (a) the heat duties of all the columns are similar (i.e., only a small energy savings is possible by adding another effect), (b) the column pressures exceed the maximum allowable pressure, (c) the column temperatures exceed the maximum utility or product decomposition temperature, (d) the sequence is more complex than desired, or (e) until some other user-imposed stopping criterion is met.

Conclusions

Existing methods for synthesizing heat-integrated distillation sequences are not sufficient when the mixtures to be separated

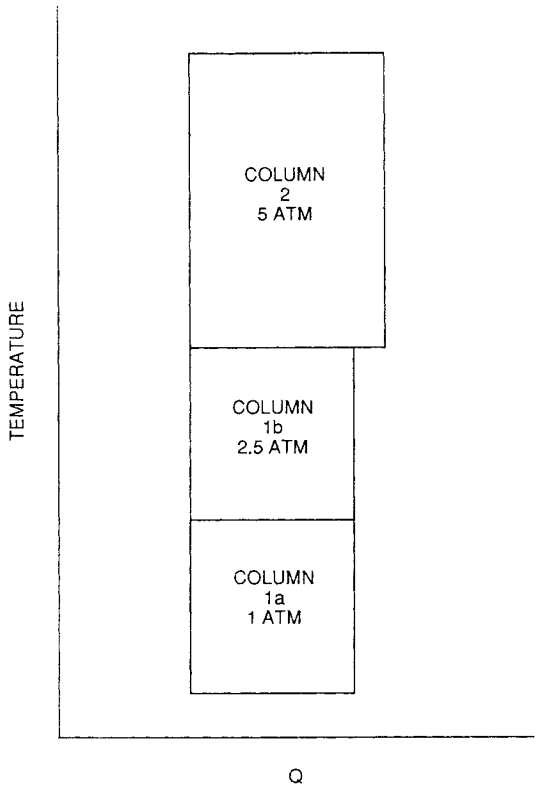

Figure 12. Structure for thermally-integrated sequence C (feed ratio = 0.55).

Predicted $\Sigma Q_{reboiler}$ = 5,750 kW assuming constant $Q\Delta T$. Columns 1a and 1b are extractive distillation columns. Column 2 is the methanol or entrainer recovery column.

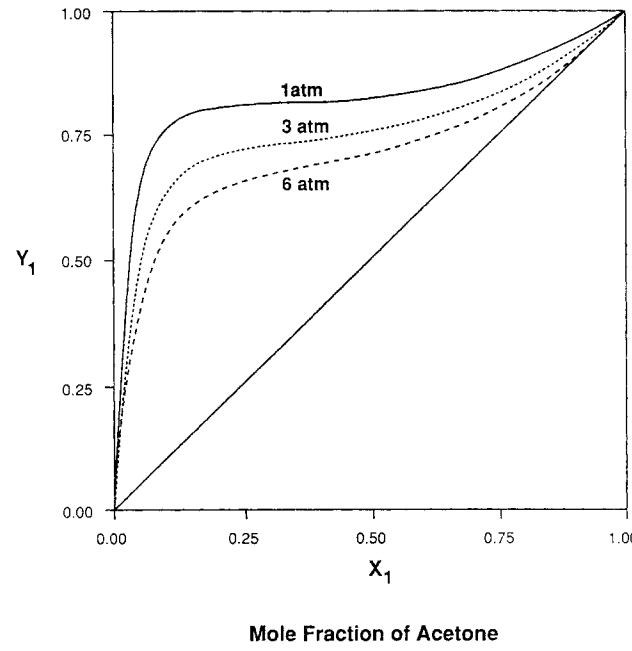

Figure 13. Binary vapor-liquid equilibrium curves for acetone-water at 1,3 and 6 atm.

Note how the tangent pinch becomes more pronounced as the pressure increases.

are nonideal or azeotropic. These techniques fail for this class of systems because increases in column pressures frequently introduce new azeotropes and distillation boundaries into the mixture, which make some separation tasks in the sequence infeasible.

The graphical thermal-integration method of Andrecovich and Westerberg (1985a) has been coupled with a bifurcation and residue-curve map analysis that accounts for the effect of pressure on the feasibility of the desired separations for nonideal and homogeneous azeotropic mixtures. The bifurcation and residue-curve map analysis identifies which, if any, separation tasks become infeasible and at which pressures. The Andrecovich and Westerberg method is then used to discriminate between the remaining thermal integration alternatives.

Contrary to the assumptions made by many previous authors, it is sometimes extremely important to include feed preheating in the thermal integration procedure. Guidelines for stream matching to preheat feed streams are given. It is also not necessary to reoptimize the sequence after changing the column pressures when the azeotropes in the mixture are not pressure-sensitive. When the azeotropes are pressure-sensitive, only those variables affected by the changing azeotropic compositions need to be reoptimized.

The appearance or disappearance of azeotropes with changing pressure (i.e., bifurcation pressures) indicates that tangent pinches will be present and conversely, the presence of tangent pinches signals that the number of azeotropes will change with pressure. Columns should not be operated at pressures near bifurcation pressures where tangent pinches will be severe.

The new thermal integration procedure for nonideal and homogeneous azeotropic mixtures is summarized in algorithmic form and is demonstrated on two separations of commercial importance. For the extractive distillation of ethanol and water using ethylene glycol, the energy consumption of the optimized nonthermally-integrated sequence is reduced by 65% to 2,700 kJ/kg by thermal integration. This is also significantly more energy-efficient than the most commonly used separation process, heterogeneous azeotropic distillation. For the extractive distillation of methanol and acetone using water, thermal integration reduces the energy consumption by 40% over the optimized nonintegrated sequence.

Acknowledgment

The authors are grateful for the research support provided by the Link Foundation in the form of an Energy Fellowship for J. P. Knapp and the financial support provided by the National Science Foundation.

Literature Cited

Andersen, H. W., L. Laroche, and M. Morari, "Effect of Design on the Control of Homogeneous Azeotropic Distillations," AIChE Meeting, San Francisco (Nov., 1989).

Anderson, E. V., "Oxygenated Fuels Mandate: Marketers Ponder Additive Strategy," *Chem. Eng. News*, **65**(31), 14 (1987).

———, "Ethyl *tert*-Butyl Ether Shows Promise as Octane Enhancer," *Chem. Eng. News*, **66**(43), 11 (1988).

Andrecovich, M. J., and A. W. Westerberg, "A Simple Synthesis Method Based on Utility Bounding for Heat-Integrated Distillation Sequences," *AIChE J.*, **31**(3), 363 (1985a).

———, "Utility Bounds for Nonconstant QΔT for Heat-Integrated Distillation Sequence Synthesis," *AIChE J.*, **31**(9), 1475 (1985b).

Barba D., V. Brandani, and G. Di Giacomo, "Hyperazeotropic Ethanol Salted-Out by Extractive Distillation. Theoretical Evaluation and Experimental Check," *Chem. Eng. Sci.*, **40**, 2287 (1985).
Black, C., "Distillation Modelling of Ethanol Recovery and Dehydration Process for Ethanol and Gasohol," *Chem. Eng. Prog.*, **76**(9), 78 (1980).
Black, C., and D. E. Ditsler, "Dehydration of Aqueous Ethanol Mixtures by Extractive Distillation," *Azeotropic and Extractive Distillation, Adv. Chem. Ser.*, No. 115, R. F. Gould, ed., ACS, Washington, DC, 1 (1972).
Collura, M. A., and W. L. Luyben, "Energy-Saving Distillation Designs in Ethanol Production," *Ind. Eng. Chem. Res.*, **27**, 1686 (1988).
Doherty, M. F., and G. A. Caldarola, "Design and Synthesis of Homogeneous Azeotropic Distillations: 3. The Sequencing of Columns for Azeotropic and Extractive Distillations," *Ind. Eng. Chem. Fund.*, **24**, 474 (1985).
Douglas, J. M., *Conceptual Design of Chemical Processes*, McGraw-Hill, New York (1988).
Douglas, L., and D. Feinberg, *Evaluation of Nondistillation Ethanol Separation Processes*, SERI/TR-231-1887, DE 83011994, U.S. Dept. of Energy (1983).
Eakin, D. E., J. M. Donovan, G. R. Cysewski, S. E. Petty, and J. V. Maxham, *Preliminary Evaluation of Alternative Ethanol/Water Separation Processes*, Battelle Pacific Northwest Laboratory, U.S. National Technical Information Service, No. PNL-3823 (1981).
Fisher, W. R., M. F. Doherty, and J. M. Douglas, "Evaluating Significant Economic Trade-Offs for Process Design and Steady-State Control Optimization Problems," *AIChE J.*, **31**(9) 1538 (1985).
Floudas, C. A., and G. E. Paules, IV, "A Mixed-Integer Nonlinear Programming Formulation for the Synthesis of Heat-Integrated Distillation Sequences," *Comput. Chem. Eng.*, **12**(6), 531 (1988).
Glinos, K., M. F. Malone, and J. M. Douglas, "Shortcut Evaluation of ΔT and $Q\Delta T$ for the Synthesis of Heat Integrated Distillation Sequences," *AIChE J.*, **31**(6), 1039 (1985).
Hindmarsh, E., and D. W. Townsend, "Heat Integration of Distillation Systems into Total Flowsheets—A Complete Approach," AIChE Meeting, San Francisco (Nov., 1984).
Julka, V., and M. F. Doherty, "A Simple Geometric Design Procedure for Multicomponent Nonideal Distillation Systems," AIChE Meeting, San Francisco (Nov., 1989).
Kakhu, A. I., and J. R. Flower, "Synthesising Heat-Integrated Distillation Sequences Using Mixed Integer Programming," *Chem. Eng. Res. Des.*, **66**(3), 241 (1988).
Katzen, R., G. D. Moon, Jr., and J. D. Kumans, "Distillation System for Motor Fuel Grade Anhydrous Ethanol," U.S. Patent No. 4,217,178 (Aug. 12, 1980).
King, C. J., et al., *Separation & Purification—Critical Needs and Opportunities*, National Research Council, National Academy Press, Washington, DC (1987).
Knapp, J. P., "Exploiting Pressure Effects in the Distillation of Homogeneous Azeotropic Mixtures," PhD Diss., Univ. of Massachusetts, Amherst (1990).
Knapp, J. P., and M. F. Doherty, "Separating Ternary Homogeneous Azeotropic Mixtures by Pressure-Swing Distillation," AIChE Meeting, New York (Nov., 1987).
Knight, J. R., "Synthesis and Design of Homogenous Azeotropic Distillation Sequences," PhD Diss., Univ. of Massachusetts, Amherst (1986).
Knight, J. R., and M. F. Doherty, "Optimal Design and Synthesis of Homogeneous Azeotropic Distillation Sequences," *Ind. Eng. Chem. Res.*, **28**(5), 564 (1989).
Ladisch, M. R., and K. Dyck, "Dehydration of Ethanol: New Approach Gives Positive Energy Balance," *Sci.*, **205**, 898 (1979).
Levy, S. G., and M. F. Doherty, "Design and Synthesis of Homogeneous Azeotropic Distillations: 4. Minimum Reflux Calculations for Multiple-Feed Columns," *Ind. Eng. Chem. Fund.*, **25**, 269 (1986).
Linnhoff, B., H. Dunford, and R. Smith, "Heat Integration of Distillation Columns into Overall Processes," *Chem. Eng. Sci.*, **38**(8), 1175 (1983).
Lynn, S., and D. N. Hanson, "Multieffect Extractive Distillation for Separating Aqueous Azeotropes," *Ind. Eng. Chem. Proc. Des. Dev.*, **25**, 936 (1986).
Messick, J. R., W. R. Ackley, and G. D. Moon, Jr., "Anhydrous Ethanol Distillation Method and Apparatus," U.S. Patent No. 4,442,903 (Dec. 27, 1983).
Meszaros, I., and Z. Fonyo, "Extensive State Optimization for Heat-Integrated Distillation Columns," *Comput. Chem. Eng.*, **12**, 225 (1988).
Minderman, P. A., Jr., and D. W. Tedder, "Comparisons of Distillation Networks: Extensively State Optimized vs. Extensively Energy Integrated," *AIChE Symp. Ser.*, **78**(214), 69 (1982).
Mix, T. J., J. S. Deweck, M. Weinberg, and R. C. Armstrong, "Energy Conservation in Distillation," *Chem. Eng. Prog.*, **74**(4), 49 (1978).
Morari, M., and D. C. Faith, III, "The Synthesis of Distillation Trains with Heat Integration," *AIChE J.*, **26**(6), 916 (1980).
Paul, J. K., ed., *Large and Small Scale Ethyl Alcohol Manufacturing Processes from Agricultural Raw Materials*, Noyes Data Corp., Park Ridge, NJ (1980).
Potter, F. L., "Ethanol and ETBE Supply and Demand Analysis—Assessing Reformulated Fuels and Environmental Regulation of Gasoline," AIChE Meeting, San Francisco (Nov., 1989).
Rathore, R. N. S., K. A. Van Wormer, and G. J. Powers, "Synthesis of Distillation Systems with Energy Integration," *AIChE J.*, **20**(5), 940 (1974).
Robinson, C. S., and E. R. Gilliland, *Elements of Fractional Distillation*, 4th ed., McGraw-Hill, New York (1950).
Ryan, P. J., and M. F. Doherty, "Design/Optimization of Ternary Heterogeneous Azeotropic Distillation Sequences," *AIChE J.*, **35**(10), 1592 (1989).
Stephanopoulos, G., B. Linnhoff, and A. Sophos, "Synthesis of Heat Integrated Distillation Sequences," *Inst. Chem. Eng. Symp. Ser.*, No. 74, 111 (1982).
Thompson, R. W., and C. J. King, "Systematic Synthesis of Separation Schemes," *AIChE J.*, **18**(5), 941 (1972).

Appendix

The costs given in this paper, as well as Knight and Doherty (1989) and Ryan and Doherty (1989), are reported in terms of total annualized cost (TAC). The TAC includes the annual operating (utility) costs and the annualized installed equipment (capital) costs. Following Douglas (1988), we use a capital charge factor of $1/3\ \text{yr}^{-1}$ to account for the time value of money to convert the capital costs to an annual basis. Unfortunately, there is an error in Douglas' derivations that leads to the incorrect equation

$$\text{TAC} = 1/3(\text{Installed Capital Costs}) + (\text{Utility Costs}) \quad \text{(A1)}$$

The correct form of this equation is

$$\text{TAC} = (\text{Installed Capital Costs}) + (\text{Utility Costs}) \quad \text{(A2)}$$

[A revised version of Douglas (1988) is forthcoming.] This error makes the absolute costs reported in Knight and Doherty (1989) and Ryan and Doherty (1989) wrong. However, the shape of the cost curves and the main conclusions are correct. Correcting the costs merely shifts the cost curves vertically. The TAC attributed to Knight and Doherty (1989) in the above text is the corrected cost for their sequence design, while the TAC attributed to Ryan and Doherty (1989) above is our best estimate of the corrected cost for their sequence.

Manuscript received Jan. 16, 1990, and revision received May 8, 1990.